Eur. Phys. J. D **11**, 213–225 (2000)

THE EUROPEAN PHYSICAL JOURNAL D

EDP Sciences
© Società Italiana di Fisica
Springer-Verlag 2000

Precise frequency measurements of I_2 lines in the near infrared by Rb reference lines

B. Bodermann, M. Klug, U. Winkelhoff, H. Knöckel[a], and E. Tiemann

Institut für Quantenoptik, Universität Hannover,Welfengarten 1, 30167 Hannover, Germany

Received 12 July 1999 and Received in final form 12 December 1999

Abstract. Frequency measurements of 16 lines of I_2 in the near infrared have been performed using different Rb frequency references: diode lasers stabilised to the Rb D1 line at 377 THz, to the Rb D2 line at 384 THz and to the $5s\ ^2S_{1/2}$–$5d\ ^2D_{3/2,5/2}$ two photon transition at 385 THz. The relative uncertainties of the measurements of $1...2 \times 10^{-10}$ are limited by the frequency stability of the laser source locked to I_2 in the case of the Rb D2 and two photon transition or by the accuracy of the Rb D1 line. The internal consistency of calibrations of iodine lines is shown to be better than 3×10^{-10} by measurements of the difference frequencies of calibrated iodine lines using four-wave mixing in laser diodes.

PACS. 33.20.Kf Visible spectra

1 Introduction

The usefulness of the iodine spectrum as frequency reference in the visible and in the NIR is well known. The iodine atlas by Gerstenkorn *et al.* [1] permits a frequency calibration in the range between 333 THz and 600 THz using Doppler-broadened lines. Doppler-free iodine lines have been used not only as a convenient tool for frequency stabilisation of lasers [2–4], but also as frequency references at a very high level of accuracy of few parts in 10^{-10} or better [5–7]. Some of them are recommended as wavelength standards by the Comité International des Poids et Mesures (CIPM) [8]. However, there was a lack of precise calibrated hyperfine iodine lines in the near infrared (NIR).

Gerstenkorn *et al.* showed, that it is possible to describe their frequency data set of 17800 iodine lines to an uncertainty level of $\delta\nu/\nu \approx 10^{-7}$ using as an adequate description the Dunham series based upon the physical model of a vibrating rotator, and to reduce the data to as few as 46 fitted molecular parameters [9]. Martin *et al.* determined molecular parameters describing the emission spectrum of iodine in the range between 222 THz and 550 THz to an uncertainty level of several 10^{-7} [10].

In our recent experiments we investigated systematically the hyperfine structure of several vibrational bands [11,12]. Additionally, we measured interferometrically the wavelength of three iodine transitions at 377.8, 379.4 and 383.6 THz with an uncertainty of $\delta\lambda/\lambda \approx 10^{-10}$ [13] and the frequency of two iodine lines at 367 THz with $\delta\nu/\nu \approx 10^{-10}$ using the difference frequency of a Ca and a CH_4 optical frequency standard [14].

In recent years optical transitions of the Rb atom have been used more and more for frequency stabilisation of diode lasers and for the realisation of secondary frequency standards in the NIR [15–17]. Barwood *et al.* used the Rb transitions $5s\ ^2S_{1/2}$–$5p\ ^2P_{1/2}$ (D1, 795 nm) and $5s\ ^2S_{1/2}$–$5p\ ^2P_{3/2}$ (D2, 780 nm) for frequency stabilisation of diode lasers and measured the frequencies of these transitions with a relative uncertainty of 1.5×10^{-10} [15,18,19]. Ye *et al.* improved the relative accuracy of the D2 line to 1.4×10^{-11} [21]. The frequency of the two-photon transition $5s\ ^2S_{1/2}$–$5d\ ^2D_{3/2,5/2}$ (778 nm) has been measured by Touahri *et al.* and Nez *et al.* with a relative accuracy of 5.2×10^{-12} ($J = 5/2$) [22] and 1.3×10^{-11} ($J = 3/2$) [16], respectively.

In this paper we will report on new absolute frequency measurements of NIR transitions of iodine, applying the precisely known Rb lines as frequency references. Additionally, by using the technique of four-wave mixing inside a diode laser, we link the different lines across the large intervals to check the internal consistency of the calibrations.

2 Frequency stabilisation to iodine lines

The frequency-stabilised diode laser has been described in detail in [4,11]. The frequency noise of the laser diode (Sharp LTO24 MD, Hitachi HL 7851 G) is reduced by more than 30 dB as compared to the free-running laser using optical feedback from a Fabry-Perot interferometer (Hollberg-setup) [23,24] leading to a fast emission linewidth of about 30 kHz. We use Doppler-free collinear saturation spectroscopy in order to resolve the hyperfine components of the rovibronic transitions of the iodine

[a] e-mail: knoeckel@iqo.uni-hannover.de

molecule. The lock of the laser to the saturation signal is achieved by the conventional $3f$-technique. To identify and to correct small electronic offsets the phase of the lock-in amplifier in the servo-loop is switched between 0° and 180° and simultaneously the sign of the locking signal is inverted in this cycle.

Five different iodine cells (named I1 to I5) were at our disposal. These were prepared and filled at the Physikalisch-Technische Bundesanstalt (PTB Braunschweig). Two of them (I1, I2), which are 50 cm long, were filled in 1994, the others (I3, I4, I5), which are 80 cm long, were filled in 1996. In the saturation setup the cells are heated to 600(30) °C and the temperature at one end of the cell was stabilised to 20(1) °C to control the vapour pressure to a value of 27.0(2.4) Pa.

The typically measured Allan standard deviation of the stabilised laser frequency is $\sigma_y(\tau) = 5 \times 10^{-12}$ for averaging times of $\tau = 100$ s, and the reproducibility of the laser frequency amounts to 10 kHz for an individual cell. However, we observed systematic frequency deviations of the same iodine transition between the different cells (probably due to different background gas pressure). A systematic study of the five iodine cells I1 to I5 showed a (1σ) standard deviation of 26 kHz, which represents the reproducibility for the use of an iodine cell prepared and operated at elevated temperatures like our cells. This value sets a lower limit for the absolute accuracy, which can be achieved by frequency calibrations reported here.

A contamination of an iodine cell with background gas usually leads to a red shift of the transition frequencies [25,26]. Because we observed the highest frequencies with the cell I5, we assumed this cell to be of higher purity. Therefore, all absolute frequencies of iodine transitions given here refer to the cell I5[1]. For the calibrations of iodine lines on the Rb D1 and D2 lines, which were performed with the older cells I1 and I2, a correction of +42 kHz was applied to the measured frequencies, corresponding to the frequency shift of −42(5) kHz of these cells compared with cell I5, which was determined in later experiments on other transitions.

3 Calibrations with the rubidium D1 line

We calibrated the transition frequencies of four iodine transitions by use of the Rb D1 line as frequency reference. The setup for frequency stabilisation of a diode laser to this Rb transition is shown in Figure 1a. It was constructed largely analogous to the one used by Barwood *et al.* for the calibration of the Rb D1 transition [15,18,19].

The output of the diode laser in a Hollberg-setup is sent through a Faraday isolator (60 dB, FI), to avoid unwanted optical feedback to the diode laser from the experiment. A part of the beam is sent through a Rb cell (pump beam), reflected back by mirror M (probe beam) and sent *via* a beamsplitter BS (50% reflectivity) to a photodiode.

[1] This is also true for the measurements reported in [13,14].

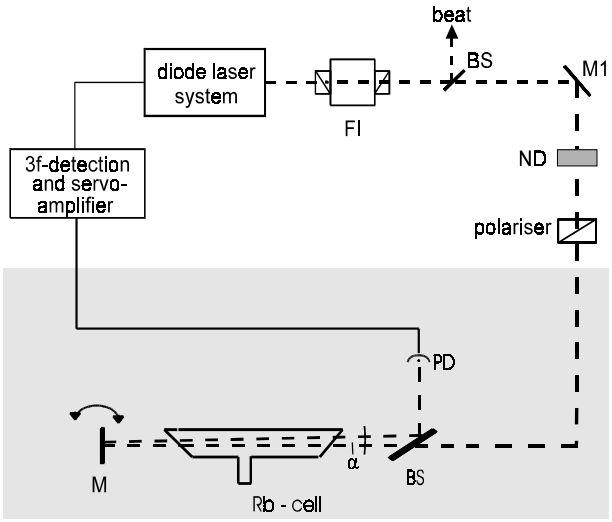

(a)

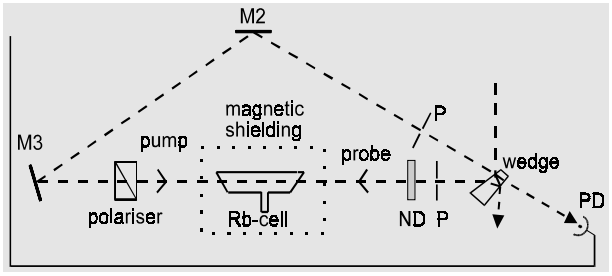

(b)

Fig. 1. (a) Experimental setup for the stabilisation of a diode laser to the Rb D1 transition. (b) setup for use of Rb D2 transition: FI: Faraday isolator, BS: beam splitter, M: mirror, ND: neutral density filter, PD: photo diode, P: pinhole.

To avoid frequency shifts due to the Zeeman effect a polariser in front of the Rb cell improves the linear polarisation of the beams, which was adjusted parallel to the earth's magnetic field. In accordance with the setup used by Barwood *et al.* the probe beam is reflected back with a small angle $\alpha = 10.0(0.5)$ mrad relative to the pump beam. The intensity of the pump and probe beam is attenuated by a neutral density filter ND to 900(90) nW/mm^2. The beams have diameters of 6 mm. The frequency of the diode laser is modulated at 3.8 kHz with a modulation amplitude of 5 MHz to provide $3f$-stabilisation of the laser frequency analogously to the iodine setup. The main part of the beam is overlapped with the output of an iodine stabilised diode laser on a fast photodiode (New Focus type 1422, bandwidth 25 GHz) for the measurement of the beat frequency between the two lasers.

For the measurements presented here the diode laser was stabilised to the component c' (transition $F_g = 3 \rightarrow F_e = 3$, of ^{85}Rb, where F_g and F_e are the total angular momentum of the ground- and the excited state, respectively), which was primarily calibrated by Barwood

Table 1. Experimental parameters for the calibrations with the Rb D1 line in comparison with those used by Barwood *et al.* [18,19]; (1) possible differences in the realisation of the Rb D1 reference in this work as compared to that of Barwood *et al.* are accounted for by an enhanced uncertainty of the reference frequency, see also text; (2) negligible if in the Barwood *et al.* experiment FM modulation with small residual AM was achieved; (3) belongs to reproducibility, the error of 0.5 mrad is statistical uncertainty, not a systematic error in the scale

parameter	Barwood *et al.*	this work	frequency uncertainty	uncertainty(1) of reproduction of reference
No of Rb-cells	2	2	< 10 kHz	≤ 50 kHz
Cell temperature	20(2) °C	26.5(1.0) °C	< 0.8 kHz	< 5 kHz
Magnetic field	30 μT	50 μT	< 8 kHz	< 8 kHz
Modulation frequ.	700 Hz	3.8 kHz	-	-
Modulation ampl.	5 MHz	5(0.5) MHz	4 kHz	(2)
Laser power	50 μW	20 μW	-	-
Beam diameter	8 mm	6(2) mm	-	-
intensity	990 nW/mm^2	880(90) nW/mm^2	5 kHz	negligible
Angle pump/probe	10 mrad	10.0(5) mrad(3)	10 kHz	(3)
total:			18 kHz	51 kHz
Allan standard deviation	4×10^{-12} ($\tau = 10$ s)	5×10^{-12} ($\tau = 20$ s)		
	1×10^{-11} ($\tau = 10^3$ s)	3×10^{-12} ($\tau = 600$ s)		
Reproducibility	44 kHz	15 kHz		

et al. [18,19]. The signal-to-noise ratio we observe of this line is about $S/N \approx 300$ for an integration time of 100 ms.

For an estimation of the accuracy of the laser frequency achieved with this setup, we investigated the dependencies of the linewidth and the line position on experimental parameters carefully. A comparison of the experimental parameters used by Barwood *et al.* and the ones in our setup is shown in Table 1. To reproduce the frequency measured by Barwood *et al.* as closely as possible we essentially used the same experimental parameters.

The measurements on the Rb D1 line were performed in spring of 1996. At this time we only had two different Rb cells, Rb1 and Rb3, at our disposal (in contrast to the other measurements below). The frequencies measured with cell Rb1 were about 20 kHz lower than the frequencies measured with Rb3. These differences, which are still below the calibration accuracy by [18] are probably due to different background gas contamination. With very conservative estimation and from the experience with the scatter of the frequencies obtained with further different cells an uncertainty budget of 50 kHz is justified.

An estimation of the quality of Rb1, Rb3 and the cells used by Barwood *et al.* can be obtained by a comparison of the observed linewidth (full width at half maximum: FWHM) of the Rb resonances. Using the experimental parameters of Table 1 we measured a FWHM of 11(1) MHz. This can be understood taking the natural linewidth of 5.7 MHz, saturation broadening and the first order Doppler effect of 4 MHz, resulting in a Voigt profile of 10 MHz width for each of the overlapping Zeeman transitions, which are shifted due to the earth's magnetic field, and an additional modulation broadening [20]. The widths were obtained by fitting a lineshape function to the observed spectra [11]. Barwood *et al.* deduced a linewidth of 12 MHz from the frequency splitting of the two outer zero crossings of the third derivative saturation signal, which, for a basic Lorentzian lineshape, is equal to the FWHM. But due to Doppler effect and frequency modulation of the laser light the detected line profile is not perfectly the third derivative of a Lorentzian, leading to an overestimation of the linewidth by this method. From line shape simulation we estimate the FWHM of the cells used by Barwood *et al.* to be 10 MHz, which is comparable to our cells.

For an investigation of possible collisionally induced frequency shifts the temperature of the Rb cell was varied between 0 °C and 40 °C. The observed frequency shift due to a variation of the background gas pressure and of the partial pressure of Rb was less than 0.8 kHz/K. In our measurement the temperature of the Rb cell was slightly higher than in the experiment of Barwood *et al.*, which could lead to a frequency difference of ≤ 5 kHz between our Rb D1 stabilised laser and the calibration by Barwood *et al.*

In accordance with the setup by Barwood *et al.* we used no magnetic shielding of the Rb cell. For a perfect linear polarisation there should be no shift of the line position because of unsymmetric Zeeman broadening, but birefringence at the cell windows or the beamsplitter can lead to a small amount of circular polarisation, which would introduce a frequency shift. We measured the frequencies of the components a, c, a' and c' with and without a magnetic μ-metal shielding of the Rb cells. For the components a and a' we obtained frequency differences of -40 kHz and

Table 2. Frequency differences of calibrated iodine lines with respect to Rb D1, component c', and transition frequencies derived.

transition	component	diff. frequency to D1, c' [kHz]	transition frequency [kHz]
P(105) 0-15	a_{14}	−18 622 175.0 (3.3)	377 087 649 355 (74)
R(205) 0-14	a_2	−1 575 867.0 (12.0)	377 104 695 663 (75)
R(113) 0-15	a_{12}	11 454 639.0 (5.0)	377 117 726 169 (74)
P(104) 0-15	a_{10}	24 731 770.2 (4.0)	377 131 003 300 (74)

−20 kHz, respectively, while for the components c and c' there was no shift observable within the reproducibility interval of 10 kHz. Therefore, we estimate the uncertainty of the frequency of the laser stabilised to component c' due to Zeeman shift to be less than 8 kHz. The reported magnetic field in the experiment of Barwood *et al.* was only 30 μT. This difference of both experiments could lead to a small frequency deviation, but not greater than 8 kHz.

For the modulation amplitudes $\Delta\nu = 5$ MHz we determined a slope of the frequency shift $\delta\nu$ of $\delta\nu/\Delta\nu = +7(1)$ kHz/MHz, resulting in a frequency uncertainty of 4 kHz due to the uncertainty of the modulation amplitude of 0.5 MHz.

The most serious frequency shifts are introduced by geometrical effects and by power shifts, which are strongly correlated, especially in this kind of saturation setup using an angle between pump- and probe beam, and which can be attributed to a combination of residual first order Doppler effect, optical pumping and light pressure [27].

For the D1 line we found the influence due to geometrical effects to be smallest, if the intensity of the pump- and the probe beam are nearly the same: $I_{\mathrm{pump}} \approx I_{\mathrm{probe}}$. The Rb frequency (of the component c') showed an approximately quadratic dependence on the angle α between pump and probe beam:

$$\nu(\alpha) - \nu(\alpha = 0) = \delta\nu(\alpha) \approx \alpha^2 \times 1.0\ \mathrm{kHz/mrad}^2.$$

Since we used $\alpha = 10.0(5)$ mrad as in the setup of Barwood *et al.*, this introduces a systematic frequency shift of 100(10) kHz with respect to the true transition frequency, but only 5 kHz uncertainty in the representation of the calibration by Barwood *et al.* For a variation of the intensity of the pump and probe beam between 440 nW/mm^2 and 880 nW/mm^2 no further significant frequency shift was observed. Therefore, the frequency uncertainty due to the power shift was estimated to be less than 5 kHz.

A comparison of the stability of the laser frequency (in terms of the Allan standard deviation) and the reproducibility reached in [18] and in our setup is also given in Table 1. Barwood *et al.* [18] reported an Allan standard deviation $\sigma_y(\tau) = 4 \times 10^{-12}$ for $\tau = 10$ s which increases slightly for increasing τ. This indicates a small frequency drift of this system. The stabilisation scheme presented here shows an Allan standard deviation of $\sigma_y(\tau) = 5 \times 10^{-12}$ for $\tau = 20$ s, and no frequency drift was observed up to $\tau = 1000$ s. Indeed, the reproducibility of our setup, tested over a month and with several readjustments of the whole setup, is a factor of three better than the one given in [18]. Reasons for this improvement are probably the use of the Faraday isolator and the additional polarizer in front of the Rb cell, which are missing in the setup described in [18]. The observed reproducibility of 15 kHz corresponds well to the estimated total uncertainty of < 18 kHz obtained from the data in Table 1.

For the frequency measurements reported here the possible frequency difference between the calibration by Barwood *et al.* and our system is taken into account by estimating an increased uncertainty for our realization of the Rb D1 reference. Therefore, the total uncertainty of the frequency of the laser stabilised to the component c' of the Rb D1 line consists of three contributions:

- from the uncertainty of the calibration in [18,19]: 60 kHz,
- the reproducibility reached in this work (see Tab. 1): 15 kHz,
- and the uncertainty from possible systematic deviations between [18,19] and this work (see Tab. 1): 51 kHz.

For the frequency of our Rb D1 standard we therefore use the value given in [18,19] with a slightly enhanced uncertainty:

$$\nu(\mathrm{Rb\ D1},\ c') = 377\,106\,271\,488(80)\ \mathrm{kHz}.$$

By measuring the beat frequencies between this Rb frequency standard and the iodine stabilised diode laser we could determine the transition frequencies of four rovibronic iodine transitions near the Rb D1 line. The frequency differences for selected iodine hyperfine components and the absolute transition frequencies are given in Table 2. Since these measurements were performed using the iodine cell I1 the absolute frequencies are corrected by +42 kHz, according to the discussion of the iodine cells above.

The hyperfine spectra of these iodine lines show a structure, which is typical for transitions with large angular momentum $J > 30$. Typical examples and the assignment of the hyperfine components can be found *e.g.* in [2,4]. The calibrated lines are practically free from overlapping hyperfine structure of other transitions.

The accuracy of this calibration is obviously limited by the accuracy of the calibration of the Rb D1 transition. In principle, the Rb D1 frequency standard should have a metrological potential comparable to the Rb D2 standard (see below). Some improvement on the reproducibility is already reached by the introduction

Table 3. Experimental parameters for the calibrations with Rb D2, compared with those used by Ye *et al.* [21], see also caption of Table 1 and text.

parameter	Ye *et al.*	this work	uncertainty of reproduction of reference
I_{pump}	3.7 μW/mm^2	3.6 μW/mm^2	740 Hz
I_{probe}	0.9 μW/mm^2	1 μW/mm^2	
Collinearity	no statement.	$\leq$ 0.5 mrad	7 kHz
Modulation amplitude	3 MHz	3(0.5) MHz	2.5 kHz
Magnetic field	< 2 μT	< 1 μT	220 Hz
Polarisation	linear, parallel	linear, parallel	
Cell temperature	*ca.* 20 °C	*ca.* 20 °C	$<$ 2.5 kHz
used cells	several	4	16 kHz
other effects			$<$ 3 kHz
total:			18 kHz
Linewidth, d/f extrapolated	7 MHz	7...7.5 MHz	

of the Faraday isolator and the additional polariser. The most severe limitation in the performance of the actual setup is probably the angle between pump and probe beam introducing a first order Doppler shift of about 100 kHz of the stabilised laser relative to the "true" transition frequency.

4 Calibration on the rubidium D2 line

The scheme we used to stabilise a diode laser to the Rb D2 line was significantly different from the D1 stabilisation. The experimental setup (Fig. 1b) was oriented on the stabilisation scheme described in [21]. The output of a diode laser system in a Hollberg-setup is sent through a Faraday isolator (60 dB), a polarizer and a wedge-shaped beamsplitter. The two reflected parts of the laser beam are used as the pump and the probe beam for the saturation spectroscopy. The pump beam is reflected by the mirrors M2 and M3, sent through another polariser and then through the Rb cell, which is put into a box of μ-metal for magnetic shielding. The probe beam is directly sent through the Rb cell anticollinearly to the pump beam, reflected by the mirrors M3 and M2 and detected on a photodiode PD. The intensity of the pump beam is adjusted by a neutral density filter ND in front of the first polariser to 3.6 μW/mm^2, the intensity of the probe beam is set by another ND to 1 μW/mm^2, close to the intensities used by Ye *et al.* [21] (see Tab. 3). Two pinholes P are used to optimise the anticollinearity of pump and probe beam. Using a diameter of 2 mm of the pinholes at a distance of 2.5 m the angle between the two beams is < 0.4 mrad, which is of the order of the beam divergence. For frequency stabilisation of the laser to the Rb resonances we used the usual $3f$-detection and stabilisation scheme mentioned above. The signal-to-noise ratio was better than 1000 for an integration time of 100 ms.

The differences between this setup and that used by Ye *et al.* are:

- Ye *et al.* used an intensity stabilised Ti:saphire-laser instead of the diode laser,
- the pump beam was chopped by an AOM and the output of the $3f$-lock-in amplifier was demodulated at the chopping frequency (double modulation scheme),
- the modulation frequency f for the $3f$-detection and the second harmonic $2f$ were notched out at the input of the $3f$-lock-in amplifier.

These differences are assumed not to introduce systematic frequency shifts between the two setups within our desired limit of accuracy.

Both Ye *et al.* and Barwood *et al.* [18,19] calibrated the d/f crossover resonance ($F_{\text{g}} = 2 \rightarrow F_{\text{e}} = 2/F_{\text{e}'} = 3$ of ^{87}Rb, F is the total angular momentum, the assignment of the hyperfine components is explained *e.g.* in [18,21]). Ye *et al.* stated a reproducibility of their laser frequency of 3 kHz, which is about 1/2000 of the observed linewidth. To reach such a high precision a careful investigation of all physical effects is necessary, which might influence the line shape and position.

The spectrum (see Fig. 2 for different pump powers) shows two peculiarities:

(1) the intensities of the crossover resonances b/f and d/f are much higher than the corresponding hyperfine components b, d and f;
(2) Ye *et al.* and Barwood *et al.* reported that the frequency of the component f ($F_{\text{g}} = 2 \rightarrow F_{\text{e}} = 3$) had a bad reproducibility and the lineshape was found to show significant asymmetries depending on the experimental parameters. Ye *et al.* attributed this behaviour to cycling effects since this transition can be considered as a two level system. In the calibrated crossover transition d/f either the pump or the probe beam is in resonance with this transition. For this reason

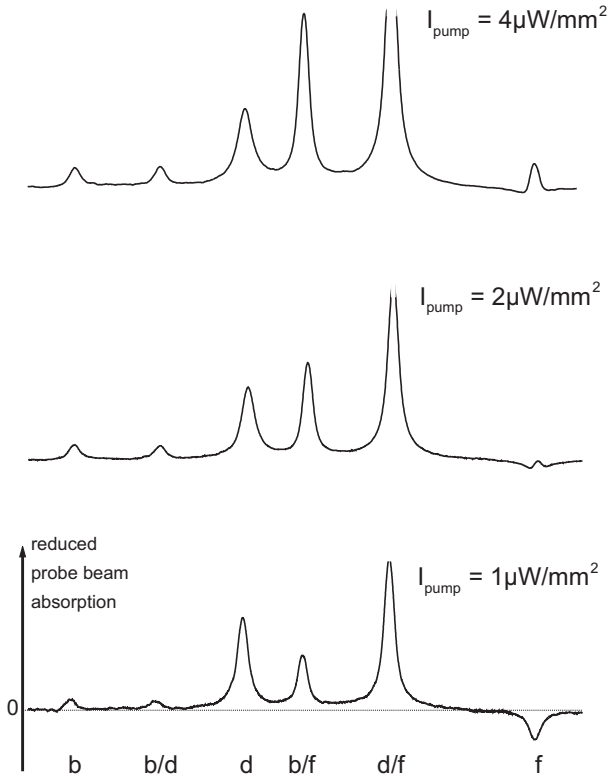

Fig. 2. Part of the saturation spectrum of the Rb D2 line. Notice the dependence of the line shape of the f component on the laser power.

it is worth to investigate this transition in more detail in order to see how cycling effects may affect the lineshape of the crossover resonance and thus also the frequency of the stabilised laser.

These peculiarities can be attributed to optical pumping. While Rb atoms, which are resonant on the transition f ($F_\mathrm{g} = 2 \rightarrow F_\mathrm{e} = 3$), undergo in the order of 100 absorption/emission cycles while crossing the laser beam (mean free path $\gg$ cell dimension), the atoms excited on the transitions b and d ($F_\mathrm{g} = 2 \rightarrow F_\mathrm{e} = 1,\ 2$) only undergo few absorption/emission cycles until the additional decay channel leads to the dark $F_\mathrm{g} = 1$ level. Thus the absorption rate for the transition f is about two orders of magnitude greater than for b and d. However, the saturation signal of the transition f is only a little bit stronger than the saturation signals for b and d, because the modified saturation intensity [28] for the transitions b and d due to the additional decay channel of the upper level is much weaker than for the transition f. The crossover resonances b/f and d/f combine the strong absorption on transition f and the weak saturation intensity of b and d. The main contribution to the crossover signal is due to the Rb-atoms with a velocity component in the direction of the laser beam, which is resonant on the transition f for the probe beam and on the transition b or d respectively for the pump beam.

The asymmetry observed for the component f is induced by at least three different effects: saturation, optical pumping and light pressure. For $I_\mathrm{pump} < 2\ \mu\mathrm{W/mm^2}$ a reversal of the saturation dip is observed (Fig. 2), caused by the influence of Zeeman pumping [29]. The linearly polarised pump beam induces an alignment of the Rb-atoms for transitions $\Delta F = \pm 1$ with a favoured population of the Zeeman sublevels with a small value of $|m_F|$. Since for these Zeeman sublevels the transition probability is greater than for the Zeeman sublevels with large values of $|m_F|$, the absorption of the probe beam is enhanced due to the Zeeman pumping of the pump beam. For small pump intensities this is the dominant effect leading to the reversal of the saturation dip. For $I_\mathrm{pump} > 2\ \mu\mathrm{W/mm^2}$ saturation becomes the dominating process, which results in reduced absorption of the probe beam. For $I_\mathrm{pump} \approx 2\ \mu\mathrm{W/mm^2}$ in particular, for which these two effects nearly cancel, a strong asymmetry of the line profile is evident. Such asymmetry, especially for closed two level systems, is induced by the influence of light pressure, which can introduce a shift of the maximum of a line profile of up to 25% of the linewidth [27]. Thus one should avoid stabilising lasers on such transitions. The influence of Zeeman pumping and light pressure on the line profile of the crossover resonance d/f is much smaller than for the component f, because of the reduced saturation intensity and of the much reduced number of absorption/emission cycles for this transition.

Table 3 contains all relevant data of the experimental conditions for the d/f component. For the intensities of the pump and the probe beam used in this experiment the influence of Zeeman pumping and light pressure on the line profile and on the frequency of the laser stabilised to this transition is quite small. A comparison of the measured frequency difference between the components d/f and f and the theoretical value, calculated from the very accurate hyperfine parameters [21], showed a deviation of only 66 kHz. For the measurements by Barwood *et al.* [18] this deviation amounted to 890 kHz.

For the frequency calibration of iodine lines we chose nearly the same experimental parameters for the Rb D2 stabilisation (compare Tab. 3) as used by Ye *et al.* [21]. The frequency dependencies of the Rb D2 stabilised laser on the different experimental parameters have been investigated carefully. For an intensity of the pump beam of $4\ \mu\mathrm{W/mm^2} < I_\mathrm{pump} < 20\,\mu\mathrm{W/mm^2}$ we measured a frequency variation of 2(1) $\mathrm{kHz\,mm^2/\mu W}$, and for $I_\mathrm{pump} > 20\ \mu\mathrm{W/mm^2}$ only 0.4(3) $\mathrm{kHz\,mm^2/\mu W}$. For all measurements the ratio between pump and probe intensity was fixed to $I_\mathrm{pump}/I_\mathrm{probe} = 4$. In [21] a value of 0.7 $\mathrm{kHz\,mm^2/\mu W}$ is reported.

In the Rb D2 stabilisation scheme four different Rb cells (Rb1–Rb4) were tested. The interval of measured linewidths (FWHM) of the crossover resonance d/f are given in Table 3. For the cells Rb1 and Rb2 we observed a slightly larger linewidth than for Rb3 and Rb4, probably due to different background gas contamination. An extrapolation to vanishing pump power and modulation amplitude results in a FWHM of 7.5(6) MHz for the cells Rb1 and Rb2 and of 7.0(6) MHz for Rb3 and Rb4. Ye *et al.* gave for their Rb cells an extrapolated FWHM

Table 4. Frequency differences of calibrated iodine lines with respect to Rb D2, and transition frequencies derived.

transition	component	diff. frequency to D2, d/f [kHz]	transition frequency [kHz]
P(70) 0-14	a_{10}	−22 789 088.4 (11.9)	384 205 192 788.6 (36)
R(188) 0-13	a_{10}	−19 508 375.6 (11.6)	384 208 473 501.4 (36)
R(117) 2-15	b_{13}	−19 054 457.0 (39.0)	384 208 927 420 (52)
P(43) 3-16	a_2	−9 373 789.0 (30.0)	384 218 608 088 (45)
P(243) 0-12	b_1	−9 169 104.0 (44.0)	384 218 812 773 (55)
R(78) 0-14	a_{10}	−5 510 359.1 (4.0)	384 222 471 517.9 (34)
P(148) 1-14	a_1	7 632 746.8 (11.7)	384 235 614 623.8 (36)

of 7 MHz [21]. For this reason our cells Rb3 and Rb4 should be of similar quality as the cells used in [21]. The cells Rb1 and Rb2 probably contained more background gas, which could result in a frequency shift of the crossover resonance d/f. Indeed we measured a frequency shift of −22(21) kHz for Rb1 and −42(21) kHz for Rb2, as compared with Rb3. Therefore, we only used the cells Rb3 and Rb4 for the frequency calibration of the iodine lines. The frequency difference between these two cells was measured to be 16(21) kHz, thus insignificant. The frequency dependence on the cell temperature for these two cells should be less than for cell Rb1 (see above), and therefore it can be estimated to be less than 0.5 kHz/K. The dependence on the modulation amplitude was found to be 2.5(5) kHz/MHz for modulation amplitudes up to 4 MHz. For greater amplitudes no further frequency shift was observed.

For a linear polarisation of the pump and the probe beams the Zeeman effect ideally causes only a line broadening, but no line shift. Since in the experiment a small amount of circular polarisation of the laser beams could be introduced, *e.g.* due to birefringence at the cell windows, the influence of a magnetic field on the line position was investigated. For this purpose the frequency of the crossover resonance d/f was measured with and without the magnetic shielding of the cell. The observed frequency shifts $\nu_{\text{unshielded}} - \nu_{\text{shielded}}$ varied between +7 kHz and +33 kHz for the different cells giving an averaged frequency shift by the earth's magnetic field of +22(10) kHz. Since magnetic fields could be suppressed by a factor of 100 with the magnetic shielding, the actual Zeeman induced frequency shift was estimated to be no more than 220 Hz.

As in the case of the Rb D1 line the most serious frequency shifts are introduced by geometrical effects. A quite strong frequency shift introduced by an angle α between pump and probe beam was already observed by Barwood *et al.* [18].

We investigated the dependence of the frequency of the components d and d/f for different values of α for the two different experimental configurations used by Ye *et al.* and by Barwood *et al.* In the latter case the first order Doppler effect introduces a frequency shift, which leads to a frequency shift of several hundred kHz for α greater than 10 mrad, and which gives rise to a bad reproducibility due to the steepness of the dependence and the experimental uncertainty of the angle α. With $\alpha < 0.4$ mrad the frequency uncertainty introduced by geometry was ≤ 7 kHz.

We measured an Allan standard deviation of $\sigma_y(\tau) = 5 \times 10^{-12}$ for $\tau = 20$ s between an iodine stabilised laser and a diode laser stabilised to the crossover resonance d/f of the Rb D2 line, limited by the stability of the iodine stabilisation. No frequency drift was observed up to $\tau = 1000$ s.

Table 3 summarises the frequency uncertainties resulting from the different experimental parameters. The total frequency uncertainty of this setup should be 18 kHz. We measured a reproducibility of the beat frequency between an iodine stabilised laser and the laser stabilised to the component d/f of the Rb D2 line of 13 kHz using only one cell and of 21 kHz using both cells Rb3 and Rb4. With an estimated reproducibility of 10 kHz for the iodine stabilisation this result is in very good agreement with the uncertainties given in Table 3.

Our representation of the Rb D2 frequency should have no systematic frequency shift to the measurements of Ye *et al.*, thus we use

$$\nu(\text{Rb D2},\, d/f) = 384\,227\,981\,877(22)\,\text{kHz}$$

where the uncertainty contains the error of 5.5 kHz of the measurement by Ye *et al.*

From the beat frequencies between the Rb D2 stabilised laser and iodine stabilised lasers seven absolute rovibronic transition frequencies could be determined. The results for selected hyperfine components are collected in Table 4. Since these measurements were performed using the iodine cell I2, the absolute frequencies are corrected by + 42 kHz, according to the discussion of the iodine cells above.

The hyperfine spectra of the transitions R(188) 0-13, R(117) 2-15, P(43) 3-16 and P(148) 1-14, which are partly overlapped by other transitions, are shown in Figure 3 in order to clarify the application of this calibration in other laboratories. The calibrated hyperfine components are indicated by arrows.

5 Calibration with the rubidium 2-photon transition $5s^2S_{1/2}$−$5d^2D_{3/2,\,5/2}$

The Rb 2-photon transition at 778 nm consists of the two fine structure components $5s\ ^2S_{1/2}$−$5d\ ^2D_{3/2}$ and

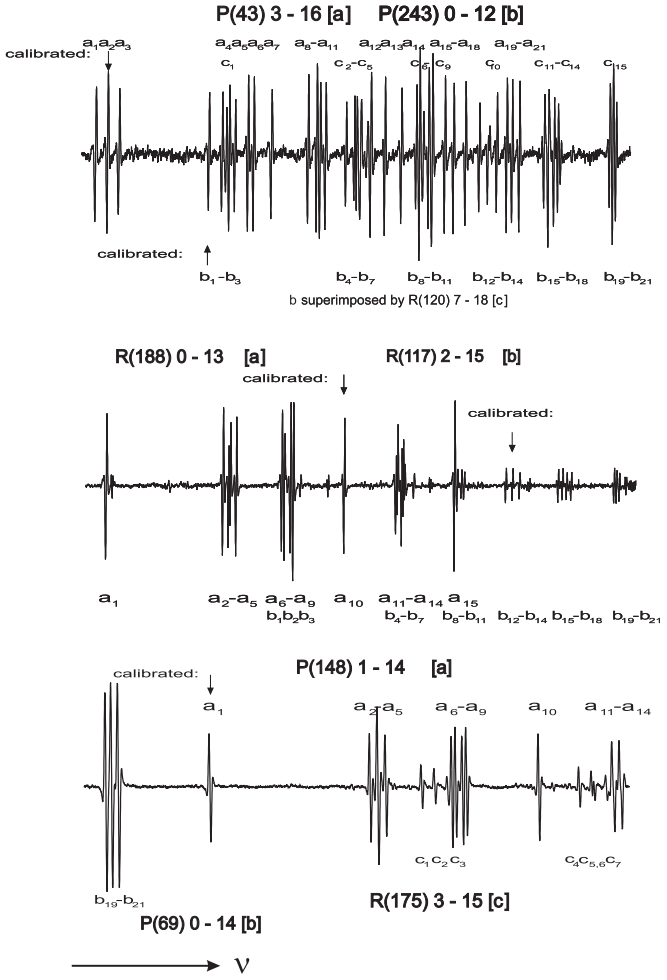

Fig. 3. Hyperfine spectra of selected iodine lines near the Rb D2 line. The calibrated lines are marked by arrows. The hyperfine transitions are numbered 1...15 for even J'' and 1...21 for odd J'', and labelled a, b, c... for the different rotational transitions.

$5s\ ^2S_{1/2}$–$5d\ ^2D_{5/2}$, which are spaced by about 45 GHz. A first precise frequency measurement of these transitions was published by Nez *et al.* [16]. The frequency of the $5s\ ^2S_{1/2}$–$5d\ ^2D_{3/2}$ was determined with an accuracy of 1.3×10^{-11}. The frequency difference between the two finestructure components was measured by Felder *et al.* [30] by use of a Schottky photodiode, leading to an accuracy of the frequency of the transition $^2S_{1/2}$–$^2D_{5/2}$ of 1.6×10^{-11}. Recently, Touahri *et al.* measured the frequency of this transition with an accuracy of 5×10^{-12} [22].

The calibrations of iodine lines presented here were performed at a time, when the calibration by Touahri *et al.* was not yet published. Therefore, the experimental setup which we used for the realisation of a Rb two photon frequency reference is very similar to the experimental setup described in [16]. The output beam of a 50 mW laser diode (Hitachi HL 7851 G) used in a Hollberg setup is sent through a 60 dB Faraday isolator to avoid optical feedback from the experiment and through a pair of anamorphic prisms to form a round beam profile with a diameter of 2 mm. A lens ($f = 500$ mm) focuses the beam into a Rb cell, and behind the cell it is reflected back by a spherical mirror ($f = 500$ mm), leading to a beam waist of about 350 μm in the center of the cell. For magnetic shielding the Rb cell is put in a box of μ-metal. The cell is heated to 90(5) °C corresponding to a Rb vapour pressure of 10^{-2} Pa. The transition is probed by fluorescence detection at 420 nm due to the radiative decay of the $5d\ ^2D$ level *via* the cascade $5d\ ^2D$–$6p\ ^2P$–$5s\ ^2S$. The fluorescence is collected by a spherical mirror ($\phi = 80$ mm, $f = 50$ mm) and imaged on a photomultiplier (R 928). A filter (Schott BG38) suppresses scattered laser light. For stabilisation of the laser its frequency is modulated (modulation frequency 5 kHz, modulation amplitude 250 kHz) and the output signal of the photomultiplier is detected at $1f$ by a lock-in amplifier. The dispersive signal is fed back *via* a servo amplifier to the piezo of the laser frequency control.

Table 5. Contributions to the linewidth of the hyperfine components of the $5s\ ^2S_{1/2}$–^2D two photon transition.

source	width [kHz]
natural linewidth	300
Zeeman broadening	< 100
wavefront mismatch	< 550
transit time	< 700
laser frequency jitter	100
pressure broadening	< 100
total:	< 1000

In the case of the $5s\ ^2S_{1/2}$–$5d\ ^2D_{5/2}$ transition the component $F_g = 2 - F_e = 4$ of the isotope ^{87}Rb was used as frequency reference because of good line intensity and the relative large frequency separation to the nearest hyperfine component. For the $5s\ ^2S_{1/2}$–$5d\ ^2D_{3/2}$ transition we used the component $F_g = 2 - F_e = 4$ (^{85}Rb) as frequency reference. The intensity of the transition $5s\ ^2S_{1/2}$–$5d\ ^2D_{3/2}$ is a factor of 20 weaker than the $5s\ ^2S_{1/2}$–$5d\ ^2D_{5/2}$ transition. However, we obtained an excellent signal-to-noise ratio of $S/N > 200$ for an integration time of 100 ms even for the weaker transition.

For the cell Rb4 we measured a FWHM of 900(100) kHz, which is larger than the value given in [16] (500 kHz), but comparable to the value measured by Biraben *et al.* [31] (1 MHz). In Table 5 the different contributions to the linewidth are summarised. The line profile for a two-photon transition was discussed in a paper by Bordé [32]. The natural linewidth amounts to 300 kHz. The Zeeman broadening for a residual magnetic field of $< 1\ \mu$T is less than 100 kHz. A residual first order Doppler broadening due to imperfect mode matching of the counterpropagating beams is estimated to be < 550 kHz. For a beam diameter of 350 μm the transit width is less than 700 kHz. In total, one expects a linewidth of 1000 kHz in accord with observation. Thus pressure broadening cannot be significant. For the other cells we measured a linewidth of 1.1 MHz (Rb3) and 2.3 MHz (Rb2), which is probably due to additional background gas in these cells. This is

Table 6. Contributions determining the uncertainty of reproducing the Rb two photon hyperfine lines, see also caption of Table 1 and text.

parameter	Felder *et al.* [30]	this work	uncertainty of reproduction of reference
intensity (AC-Stark)	10 mW/mm^2	125 mW/mm^2	10
cell (FWHM*)	500 kHz	565 kHz	20
geometry	-	< 1 mrad	< 3
modulation	500 kHz	500 kHz	< 3
pressure (temperature)	≈ 90 °C	90(5) °C	1.5
total:			23

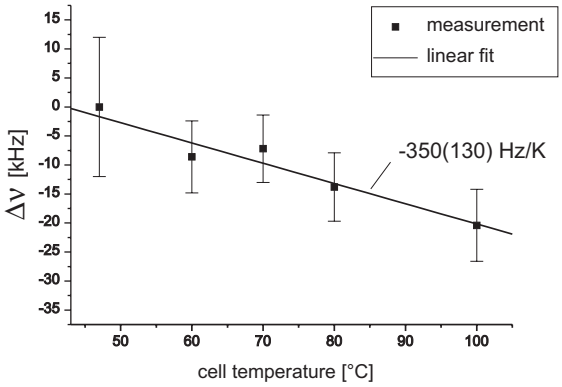

Fig. 4. Frequency shift of the $F_g = 2 \rightarrow F_e = 4$ hyperfine component of the Rb $5s\ ^2S_{1/2}$–$5d\ ^2D_{3/2}$ two photon transition as a function of the cell temperature.

consistent with our observations in connection with the calibrations using the RB D2 line, see above. For final frequency measurements we therefore used only cell Rb4.

Nez *et al.* [16] observed frequency shifts due to laser intensity (AC Stark-effect). In our system we measured an intensity dependent frequency shift of -0.2 kHz mm^2/mW in very good agreement with [30]. No frequency dependence on the modulation amplitude or on the geometry was observed. In contrast to the results in [16] we found a small temperature dependence of the frequency, which is shown in Figure 4. For cell Rb4 we derived a value of $-350(130)$ Hz/K. Table 6 collects all sources of uncertainty. The total uncertainty of the realisation of the 2-photon Rb reference is estimated to 23 kHz. Because of the higher laser intensities the frequency of our system is shifted to the red in comparison to the system of Nez *et al.* Therefore, we applied a correction of $-25(10)$ kHz derived from the experimentally determined shift to the frequencies given in [16]. For frequency calibration of the iodine lines we used as references:

$\nu(^{85}\mathrm{Rb};\ 5s\ ^2S_{1/2}\text{–}5d\ ^2D_{3/2};\ F_g = 2\text{–}F_e = 4)$:

385 242 216 338 (23) kHz,

$\nu(^{87}\mathrm{Rb};\ 5s^2S_{1/2}\text{–}5d\ ^2D_{5/2};\ F_g = 2\text{–}F_e = 4)$:

385 284 566 348 (24) kHz.

We measured the absolute frequencies of five rovibronic transitions of $^{127}I_2$ around 778 nm. The beat frequencies for selected hyperfine components and the resulting transition frequencies of the iodine lines are given in Table 7. The frequency of the R(139) 1-14 was referenced to both Rb lines, so that we can determine the frequency difference between these two lines of Rb. We obtain a value of 42 350 004.2(88) kHz, which is in very good agreement with the value of 42 350 010(6) kHz measured by Felder *et al.* [30].

The hyperfine spectra of the transitions P(19), R(18) and R(16) are shown in Figure 5. The calibrated hyperfine components are indicated by arrows. The R(26) 0-14 and R(139) 1-14 show the typical, often published structure of transitions with high values of J, thus no guide for identifying the calibrated component seems to be necessary.

6 Check of the consistency using four wave mixing in laser diodes

Nondegenerated four-wave mixing (FWM) in laser diodes allows the phase coherent bisection or extrapolation of frequency intervals up to few THz [33,34]. We used this method for a check of the internal consistency of different calibrations of iodine lines in the NIR described in this paper or in earlier publications [13,14].

The experimental setup is shown in Figure 6. The output beams of two iodine stabilised diode lasers (A, B) are superimposed and coupled into another laser diode LD_M without any optical frequency stabilisation. For a frequency difference $\delta\nu = \nu_B - \nu_A$, FWM in LD_M leads to mixing products at the frequencies $\nu_M = \nu_B \pm \delta\nu$ and $\nu_M = \nu_A \pm \delta\nu$. The output of LD_M can be analysed by a scanning Fabry-Perot interferometer and a spectrograph. The most sensitive and precise detection of the mixing products is achieved by heterodyne detection using another laser system (LO) as local oscillator. For this purpose a part of the output beam of LD_M and laser LO are superimposed on an avalanche photodiode (APD, bandwidth 1.2 GHz). The beat note of the mixing product ν_M and the local oscillator can be detected by a spectrum analyser or counted by a frequency counter. To improve

Table 7. Calibrated iodine lines relative to the Rb $5s\ ^2S_{1/2}$–^2D two photon transition.

transition	component	difference to ^{85}Rb $5s\ ^2S_{1/2}$–$5d\ ^2D_{3/2}$, $F_g = 2 \rightarrow F_e = 4$ [kHz]	difference to ^{87}Rb $5s\ ^2S_{1/2}$–$5d\ ^2D_{5/2}$, $F_g = 2 \rightarrow F_e = 4$ [kHz]	frequency [kHz]
P(19) 0-14	a_{13}	−23 691 345 (17)		385 218 524 993 (38)
R(26) 0-14	a_{10}	−8 778 157.3 (2.5)		385 233 438 181 (34)
R(139) 1-14	a_{13}	24 513 384.1 (6.7)	−17 836 620.1 (5.7)	385 266 729 725 (35)
R(18) 0-14	a_{10}		7 506 117.6 (8.0)	385 292 072 466 (35)
R(16) 0-14	a_{10}		18 134 356.8 (8.5)	385 302 700 705 (35)

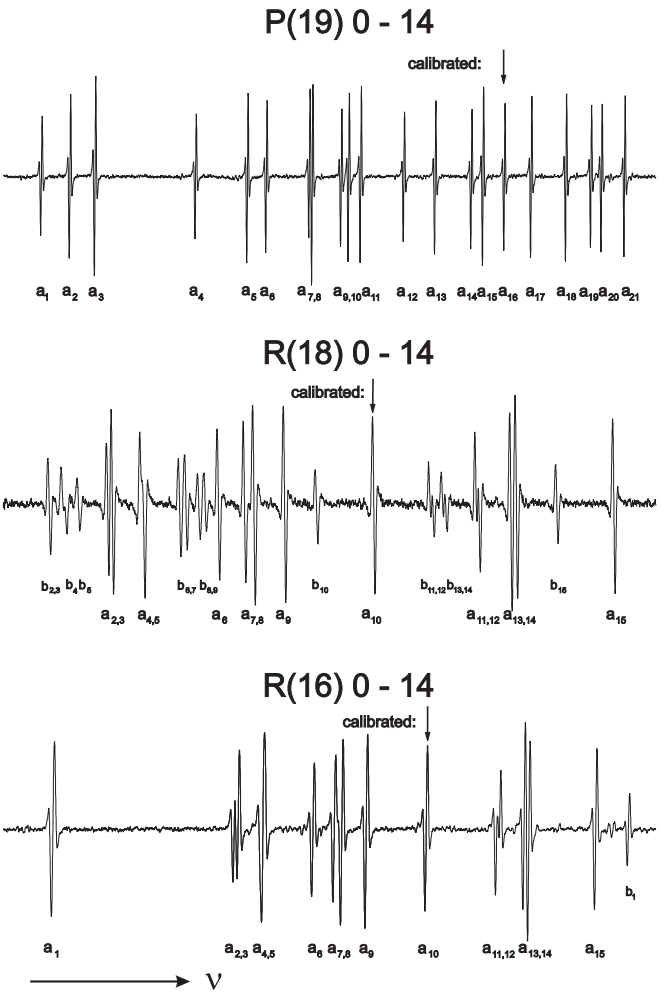

Fig. 5. Hyperfine spectra of three of the calibrated iodine lines near the Rb two photon transition $5s\ ^2S_{1/2}$–$5d\ ^2D_{3/2}$ near 778 nm.

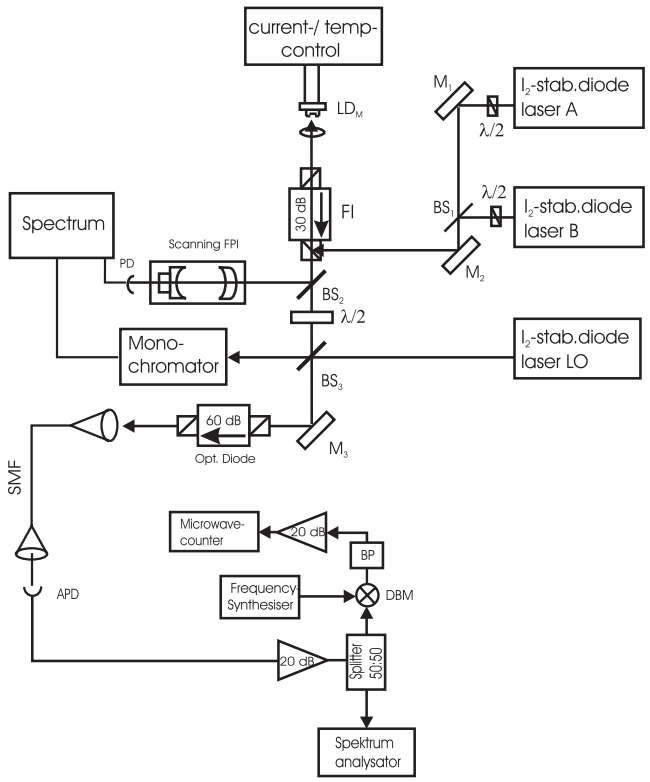

Fig. 6. Experimental setup for optical interval bisection/extrapolation using four wave mixing in a laser diode, details see text.

the signal to noise ratio for the counting the detection bandwidth is reduced. For this purpose the beat note is mixed with the signal of a microwave frequency synthesizer (HP 8660 C) in a double balanced mixer DBM, the output of which is filtered by two passband filters (center frequency 60 MHz, 3 dB bandwidth 30 MHz), amplified and fed into the frequency counter.

For an efficient four-wave mixing in LD_M both frequencies of the pump fields ν_A and ν_B and the mixing product ν_M have to coincide with resonances of the cavity created by the chip of LD_M. Therefore, the intervals $\delta\nu$ which can be used in this scheme, have to be close to integer multiples multiple of the mode spacing of the laser chip ($\approx$ 145 GHz). This restricts the general application and even for a dense spectrum like that of I_2 it is difficult to find adequate transition pairs.

Figure 7 shows schematically how we used this method to link the frequencies of three iodine lines, which were calibrated by different methods.

In a first step laser A is stabilised to the P(87) 0-14. The frequency of this line is determined by a measurement of the beat frequency between laser A and a laser stabilised

Table 8. Frequencies of iodine lines calibrated by four wave mixing and comparison with directly calibrated lines. * measured in more than one step.

transition	comp.	frequency by FWM [kHz]	frequency by 2-photon calibration [kHz]	difference FWM – 2-phot. [kHz]
R(56) 0-14	a_{10}	384 783 612 796 (117)		
	a_{15}	384 783 907 243 (118)		
P(31) 0-14	a_7	385 074 236 875 (144)		
	a_4	385 074 117 864 (138)		
P(19) 0-14	a_{14}	385 218 585 638 (140)	385 218 585 566 (40)	72
	a_{16}	385 218 641 143 (140)	385 218 641 068 (40)	75
P(164) 0-13	a_1	385 363 327 704 (242)	385 363 327 783 (56)*	−79
	a_{10}	385 363 916 052 (242)	385 363 916 113 (55)*	−61
	a_{15}	385 364 210 288 (243)		

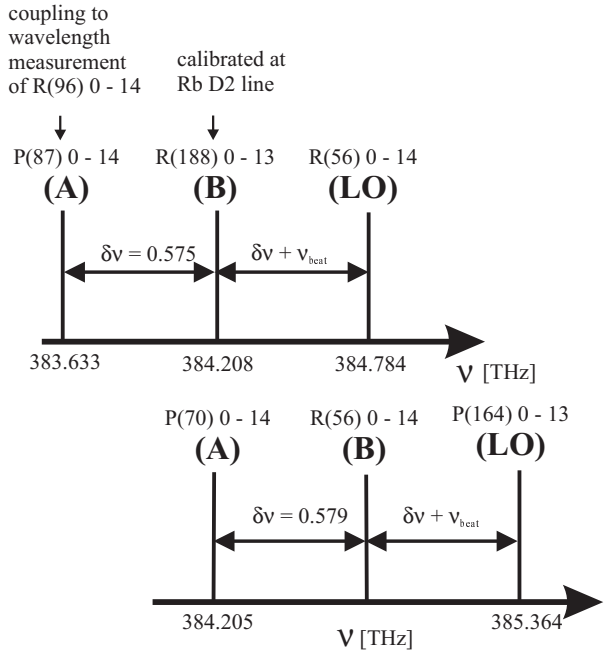

Fig. 7. Linkage scheme of measuring the three calibrated iodine lines R(96) 0-14, R(188) 0-13/P(70) 0-14 and P(164) 0-13. All frequencies are given in THz.

to the R(96) 0-14, the frequency of which is known from wavelength measurement [13]. Laser B is stabilised to the R(188) 0-13, which is calibrated by frequency comparison with the Rb D2 line (see above). FWM of these two fields in LD_M creates a mixing product of the frequency

$$\nu_M = 2\nu_B - \nu_A = \nu_B + \delta\nu.$$

The local oscillator LO is stabilised to an iodine transition (the R(56) 0-14) near to ν_M. Thus the frequency of the R(56) 0-14 could be determined by measurement of the beat frequency between LO and the mixing product.

In a second step we stabilised laser B to the R(56) 0-14 and laser A to the P(70) 0-14 (which is likewise calibrated by frequency comparison with the Rb D2 line, see above), leading to a mixing product with $\nu_M \approx \nu_{P(164)0-13}$. By measurement of the beat frequency between the mixing product and the laser LO stabilised to the line P(164) 0-13 we determined the frequency of this iodine transition. Thus this frequency is derived from the Rb D2 line and the wavelength calibration in [13].

The frequency of the P(164) 0-13 line is also determined by measurement of the difference frequency to the R(16) 0-14, which is calibrated at the Rb 2-photon transition (see above). Since this difference frequency is about 61 GHz and our detection bandwidth is limited to 25 GHz we determined this frequency difference stepwise using two intermediate iodine lines, the R(138) 1-14 and the R(240) 0-12

$$\nu_{P(164)0-13,\,a10} - \nu_{R(240)0-12,\,a10} = 16\,324\,846(27)\ \text{kHz}$$
$$\nu_{R(240)0-12,\,a10} - \nu_{R(138)1-14,\,a10} = 24\,845\,370(30)\ \text{kHz}$$
$$\nu_{R(138)1-14,\,a10} - \nu_{R(16)0-14,\,a10} = 20\,045\,192(12)\ \text{kHz}$$

total :

$$\nu_{P(164)0-13,\,a10} - \nu_{R(16)0-14,\,a10} = 61\,215\,408(42)\ \text{kHz}.$$

Additionally, we measured the frequencies of the P(31) 0-14 at 385.074 THz by bisection of the frequency intervals $\nu_{P(164)0-13} - \nu_{R(56)0-14}$ and the P(19) 0-14 at 385.218 THz by bisection of $\nu_{P(164)0-13} - \nu_{P(31)0-14}$.

Table 8 lists the frequencies of the iodine lines, which are determined by FWM in connection with Rb D2 and wavelength calibration or by the Rb 2-photon calibration. The agreement between these independently measured values is good within the experimental errors, indicating that the consistency between the three different calibration methods is at least ±100 kHz. The small deviations of $\approx +75$ kHz for the P(19) and ≈ -70 kHz for the P(164) line might be attributable to insufficient corrections of pressure shifts between the different iodine cells used for the stabilisation of the laser systems A, B and LO in Figure 6. This systematic source of error in such a measurement would be reduced by applying a single iodine cell for frequency stabilisation of all three laser systems.

The most important difficulties in the method of FWM in laser diodes for frequency measurements are the relatively low signal-to-noise ratio for the heterodyne detection of the weak mixing products and the restriction of the useable frequency intervals to the free spectral range of the mixing laser diode. While the first problem could be weakened by a further reduction of the detection bandwidth (*e.g.* by use of a tracking oscillator [14]), a solution of the second problem could possibly be the use of an antireflection coated laser diode in an external tuneable resonator, or the application of different types of laser diodes with different chip lengths, so that several different FSR (free spectral range) multiply the chances of finding pairs of transitions.

7 Discussion and outlook

With the present results and from earlier publications [13,14] there are now several precisely known iodine lines in the NIR available, which can be used as frequency references in this spectral region in addition to the Rb D1 and D2 lines and the 2-photon transition at 778 nm. The advantages of the iodine molecule as frequency reference are the very weak influence of external fields on the transition frequencies, the insensitivity against misalignment of pump and probe beam and the manifold of possible frequency references using a single molecular species. The main disadvantage in the NIR lies in the low thermal population of the vibrational levels of I_2, demanding for a quite high iodine pressure and the use of relatively long cells, which have to be heated to about 700 K. Besides a relatively low signal-to-noise ratio (as compared with iodine lines in the visible), we observe frequency shifts of a few 10 kHz between different cells caused by different background gas pressure. Additionally, due to the heating an enhanced aging of the cells attributed to permeation of air through the cell walls may appear. But over a period of two years we observed only changes of these pressure shifts between different cells of up to 50 kHz for that cell, which was mostly used and which was heated to 600 °C. For the cells temperatured to only 400 °C this change was < 20 kHz.

This work is also a study about the applicability of the reference lines of Rb. The limits by geometry, laser intensity and preparation of the cells are clarified. For further improvements the Rb D1 line should be recalibrated. Of the three Rb resonances used as frequency references the two-photon transition at 778 nm shows the best performance, which is limited by the quality of the Rb cells used. For a calibrated cell of better quality the accuracy of such a frequency standard could reach a level of few kHz. For the case of the Rb D lines, however, we observed a relative large dependence on the geometry of the saturation setup. This limits the achievable accuracy of such a frequency standard to about 10 kHz. The calibrations of iodine lines on the two photon transition and on the Rb D2 line are presently limited by the reproducibility of the iodine standards (see above), while for the measurements at 795.5 nm the limitation is the accuracy of the calibration of the Rb D1 line [19].

The set of precisely known iodine lines in the NIR will be the basis for a new determination of very accurate molecular parameters, which allow a very good interpolation of the transition frequencies of other, not measured lines in this spectral region. We determined a set of parameters describing the range between 778 nm and 815 nm with a relative accuracy of 3×10^{-10}. The results will be published elsewhere [35].

The performance of frequency stabilisation to iodine lines in the NIR is limited due to the low thermal population of the ground state vibrational levels leading to a low signal-to-noise ratio and to a pressure broadening of several MHz. An efficient population transfer to the vibrational levels needed for the NIR transitions would improve the signal-to-noise ratio and allow a reduction of gas pressure and thus of the linewidth, so that an improvement of the reproducibility of about one order of magnitude could be expected. Such a population transfer can be realised by coherent optical pumping schemes like a Raman arrangement, but the simple table top setup of the present realisation will be lost.

An interesting possibility for an extension of the calibrated spectral range to higher frequencies is given by the 2-photon-2-colour transition $5s\ ^2S_{1/2}-5d\ ^2D_{3/2,5/2}$ of the Rb atom. If the frequency of one of the exciting lasers is known (*e.g.* by stabilisation to a calibrated iodine transition) the frequency of the second laser can be derived, since the total energy of this transition is very accurately known from the measurements of the 2-photon transition at 778 nm [16,22].

We thank M. Brennecke for the filling of the iodine cells and H.R. Telle for fruitful advice. The contructive remarks of the referees on an earlier version of this paper were very helpful. This work was supported by Deutsche Forschungsgemeinschaft.

References

1. S. Gerstenkorn, P. Luc, *Atlas du spectre d'absorption de la molecule d'iode*, Laboratoire Aimé Cotton, CNRS II, Orsay (France), 14 000–15 600 cm^{-1} (1978), 15 600–17 600 cm^{-1} (1977), 17 500–20 000 cm^{-1} (1977); S. Gerstenkorn, J. Verges, J. Chevillard, *Atlas du spectre d'absorption de la molecule d'iode*, Laboratoire Aimé Cotton, CNRS II, Orsay (France), 11 000–14 000 cm^{-1} (1982).
2. A. Arie, R.L. Byer, Opt. Commun. **111**, 253 (1994).
3. A. Morinaga, K. Sugiyama, N. Ito, J. Helmcke, J. Opt. Soc. Am. B **6**, 1656 (1989).
4. S. Kremser, B. Bodermann, H. Knöckel, E. Tiemann, Opt. Commun. **110**, 708 (1994).
5. O. Acef, J.J. Zondy, M. Abed, D.G. Rovera, A.H. Gérard, A. Clairon, Ph. Laurent, Y. Millerioux, P. Juncar, Opt. Commun. **97**, 29 (1993).
6. S.L. Cornish, Y.-W. Liu, I.C. Lane, P.E.G. Baird, G.P. Barwood, P. Taylor, W.R.C. Rowley, J. Opt. Soc. Am. B **17**, 6 (2000).
7. P. Jungner, M.L. Eickhoff, S.D. Swartz, J. Ye, J.L. Hall, SPIE **2378**, 22 (1995).

8. T.J. Quinn, Metrologia **30**, 523 (1994).
9. S. Gerstenkorn, P. Luc, J. Phys. France **46**, 867 (1985).
10. F. Martin, R. Bacis, S. Churassy, J. Verges, J. Mol. Spectrosc. **116**, 71 (1986).
11. H. Knöckel, S. Kremser, B. Bodermann, E. Tiemann, Z. Phys. D **37**, 43 (1996).
12. B. Bodermann, H. Knöckel, E. Tiemann (to be published).
13. B. Bodermann, G, Bönsch, H. Knöckel, A. Nicolaus, E. Tiemann, Metrologia **35**, 105 (1998).
14. B. Bodermann, M. Klug, H. Knöckel, E. Tiemann, T. Trebst, H.R. Telle, Appl. Phys. B **67**, 95 (1998).
15. G.P. Barwood, P. Gill, W.R.C. Rowley, J. Phys. E **21**, 966 (1988).
16. F. Nez, F. Biraben, R. Felder, Y. Millerioux, Opt. Commun. **102**, 432 (1993).
17. M. Breton, P. Tremblay, C. Julien, N. Cyr, M. Têtu, C. Latrasse, IEEE Trans. Instrum. Meas. **44**, 162 (1995).
18. G.P. Barwood, P. Gill, W.R.C. Rowley, Appl. Phys. B **53**, 142 (1991).
19. G.P. Barwood, P. Gill, W.R.C. Rowley, SPIE **1837**, 262 (1992).
20. J. Helmcke, F. Beyer-Helms, PTB-Me **17**, 85 (1977).
21. J. Ye, S. Swartz, P. Jungner, J.L. Hall, Opt. Lett. **21**, 1280 (1996).
22. D. Touahri, O. Acef, A. Clairon, J.-J. Zondy, R. Felder, L. Hilico, B. de Beauvoir, F. Biraben, F. Nez, Opt. Commun. **133**, 471 (1997).
23. B. Dahmani, L. Hollberg, R. Drullinger, Opt. Lett. **12**, 876 (1987).
24. H. Li, H.R. Telle, IEEE J. Quant. Electron. **18**, 257 (1989).
25. F. Spieweck, IEEE Trans. Instrum. Meas. **IM-34**, 246 (1985).
26. S. Picard, Metrologia **26**, 235 (1989).
27. R. Grimm, J. Mlyneck, Appl. Phys. B **49**, 179 (1989).
28. M.D. Levenson, *Introduction to Nonlinear Laser Spectroscopy* (Academic Press, 1982).
29. O. Schmidt, K.-M. Knaak, R. Wynands, D. Meschede, Appl. Phys. B **59**, 167 (1994).
30. R. Felder, D. Touahri, O. Acef, L. Hilico, J.J. Zondy, A. Clairon, B. de Beauvoir, F. Biraben, L. Julien, F. Nez, Y. Millerioux, SPIE **2378**, 52 (1995).
31. F. Biraben, M. Inguscio, F. Martin, F. Pavone, Laser Phys. **4**, 349 (1994).
32. Ch.J. Bordé, C.R. Acad. Sci. B **282**, 341 (1976).
33. C. Koch, H.R. Telle, Opt. Comm. **91**, 371 (1992).
34. C. Koch, H.R. Telle, J. Opt. Soc. Am. B **13**, 1666 (1996).
35. B. Bodermann, H. Knöckel, E. Tiemann (to be published).